

Chapter 1

Chiral Electroweak Currents in Nuclei

D.O. Riska

*Finnish Society of Science and Letters, Helsinki, Finland, and
The Cyprus Institute, Nicosia, Cyprus*

R. Schiavilla

*Theory Center, Jefferson Lab, Newport News, Virginia, and
Physics Department, Old Dominion University, Norfolk, Virginia*

The development of the chiral dynamics based description of nuclear electroweak currents is reviewed. Gerald E. (Gerry) Brown's role in basing theoretical nuclear physics on chiral Lagrangians is emphasized. Illustrative examples of the successful description of electroweak observables of light nuclei obtained from chiral effective field theory are presented.

1. Introduction

The phenomenological success of the systematic application of chiral effective field theory (χ EFT) to the electromagnetic and weak observables of light nuclei in the mass range $A = 2$ – 10 has been remarkable. Here the background and early application of chiral Lagrangians to nuclear current operators, and Gerry Brown's role as an initiator of this approach are reviewed in the next section. The third and fourth sections contain a summary of the present stage of the χ EFT approach and a set of illustrative examples of its application to nuclear electroweak observables.

2. Historical Perspective

2.1. *Gerry Brown's early work with chiral Lagrangians*

Gerry Brown was one of the first physicists to appreciate the utility of effective chiral Lagrangians in theoretical nuclear physics. In the late 1960s he

planned a major effort to derive a realistic nucleon-nucleon (NN) interaction model from meson exchange, as he saw that the pair suppression built into Weinberg's non-linear chiral Lagrangian for the pion-nucleon interaction [1] might solve the over-binding problem, which the two-pion exchange interaction described with the conventional pseudoscalar pion-nucleon coupling model inevitably led to. That a realistic description of the nucleon-nucleon amplitude could be constructed in this way was then demonstrated by Brown and Durso [2] and Chemtob, Durso, and Riska [3].

In parallel with this development Chemtob and Rho derived expressions for the exchange current contributions to the electromagnetic and axial two-nucleon current operators that arise from the effective chiral Lagrangians for pion and vector meson exchange [4]. The ρ -meson exchange interaction complements the pion exchange one by counteracting the strong tensor component of the latter and improving the interaction models of Refs. [2, 3]. Concurrently, it enhances the effects of the long range electromagnetic pion exchange current.

Gerry Brown's interest in the role of exchange currents in nuclei was stimulated by Chemtob and Rho's estimate of the axial exchange current enhancement of the Gamow-Teller matrix element in Tritium β -decay [5]. He suggested that the D-state components in the trinucleon wave functions, even if small, could enhance the calculated value. This was illustrated with a schematic model for the those components [6].

The axial exchange current is related to the NN interaction indirectly through the partially-conserved axial current (PCAC) relation to the pion-production operator. The form of the electromagnetic exchange current is in contrast directly constrained by the NN interaction through the continuity equation [7, 8]. The first demonstrations that electromagnetic exchange currents could play a significant role in nuclear observables were in fact related to those. In 1971 Gerry Brown's attention was drawn to the fact the well measured total cross section for capture of thermal neutrons on protons—the process ${}^1\text{H}(n, \gamma){}^2\text{H}$ —could not be fully explained by the sum of the neutron and proton magnetic moments. He asked one of us (DOR) to take into account the pion exchange current operators derived by Chemtob and Rho [4]. The result was that the exchange current contribution can account for the $\sim 10\%$ difference between the calculated and the experimental value for the cross section [9]. The key part of the pion exchange current operator was related to the chiral Lagrangian for the pion-nucleon interaction. A smaller, nevertheless significant, effect was due to the pion exchange operator, which involved intermediate Δ resonances [10].

2.2. *The sequel*

It was soon afterwards shown that the experimental values of the ${}^3\text{H}$ and ${}^3\text{He}$ magnetic moments could also be almost fully accounted for in the same way with realistic wave functions [11]. Moreover it was found that the pion exchange current contribution could provide about one half of the cross section for capture of thermal neutrons on ${}^2\text{H}$ [12]. Later it was shown that the exchange current contribution to the calculated cross section for thermal neutron capture on ${}^3\text{He}$ is about 5 times larger than that from the sum of the three nucleon magnetic moments [13]. Finally it was shown that the cross section for radiative neutron capture on ${}^3\text{He}$ is almost totally due to the exchange current contribution [14].

While the strength of the NN interaction scales with the mass of the exchanged system, the meson exchange magnetization operator scales with the inverse mass of the exchanged system [15]. This makes the relative contribution of short-range mechanisms to the matrix elements of the exchange current operators much weaker than to the matrix elements of the interaction. The calculated cross section for backward electro-disintegration of the deuteron, which is very strongly dependent on the electromagnetic exchange currents, illustrates this well [16]. In this reaction the matrix element of the single-nucleon current operators changes sign at fairly low momentum transfer and therefore the cross section near that zero is built up entirely from the exchange current contribution. In this case the cross section obtained with the pion-exchange current alone is quite similar to that calculated later with wave functions that are consistent with a realistic phenomenological interaction model [17]. In the case of the magnetic form factors of the trinucleons there is a similar destructive interference between the matrix elements of the single-nucleon current operators for the S- and D-state components of the wave functions [18], with the consequence that the exchange current contribution is very large [19]. With only the single-nucleon current operator, the calculated magnetic form factors of the trinucleons would have zeroes at fairly low values of momentum transfer, in disagreement with experiment. This has later been demonstrated with improved wave functions and exchange current operators that satisfy the continuity equation with realistic interactions [20]. In larger nuclei the main features in elastic and transition electromagnetic form factors are due to the shell structure. Even so, it has been shown that in the case of Li, the inclusion of the exchange current contribution does markedly improve the agreement with experiment for these form factors, once the interaction

currents are consistent with wave functions corresponding to realistic interaction models [21]. The effect is smaller in ^{12}C [22] and in ^7Li , ^9Be and ^{10}B [23].

In the examples above, it is the isovector part of the pion exchange current operator, which is numerically most important. In the case of the magnetic form factor of the deuteron, only the isoscalar part of the pion exchange current contributes, and the most important term in that operator involves a $\rho\pi\gamma$ transition. Without this exchange current operator the calculated magnetic moment of the deuteron would have a node close to momentum transfer values $\sim 6 \text{ GeV}/c$, in disagreement with experiment [17, 24]. Since the $\rho\pi\gamma$ exchange current is transverse, its form is not constrained by the NN interaction by the continuity equation. Its longer range form can however be determined in the Skyrme model approach by the chiral anomaly [25, 26].

While the two-nucleon exchange current operators give large contributions to nuclear electromagnetic observables, it has been demonstrated that the three-nucleon exchange current operators that are associated with two-pion exchange with pion scattering off an intermediate nucleon, give but very small contributions to the magnetic form factors of the trinucleons [27]. The remarkably successful nuclear phenomenology based on the simple pion exchange operators that are related to the lowest order chiral Lagrangian for the pion-nucleon interaction has later been explained within the context of χEFT [28].

2.3. The axial exchange current

The role of the pion exchange axial exchange current was first considered for the case of the Gamow-Teller transition in the β -decay of Tritium. Those results were reaffirmed with more accurate wave functions [29]. Gari and Huffman noted that this axial exchange current also contributes a small enhancement of the cross section for the basic solar burning reaction $^1\text{H}(p, e^+ \nu_e)^2\text{H}$ [30]. This was confirmed by Dautry, Rho, and Riska in a study of muon absorption in the deuteron $^2\text{H}(\mu^-, \nu_\mu)nn$ with an improved version of the axial exchange current operator, which was checked for consistency against the P-wave piece of the cross section for the reaction $^1\text{H}(p, \pi^+)^2\text{H}$ near threshold [31]. The same Hamiltonian was then used to calculate the matrix elements for the solar neutrino processes $^1\text{H}(p, e^+ \nu_e)^2\text{H}$ and $^1\text{H}(p e^-, \nu_e)^2\text{H}$ as well. A later calculation, with wave functions obtained from the realistic Argonne v_{14} NN interaction [32] of the

weak proton capture reactions ${}^1\text{H}(p, e^+ \nu_e){}^2\text{H}$ and ${}^3\text{He}(p, e^+ \nu_e){}^4\text{He}$ normalized axial exchange current operator against the known rate of the Gamow-Teller component in Tritium [33]. The result was that the exchange current increased the cross section of the reaction ${}^1\text{H}(p, e^+ \nu_e){}^2\text{H}$ by 1.5 % and that of the reaction ${}^3\text{He}(p, e^+ \nu_e){}^4\text{He}$ by almost a factor 5. The axial exchange current contributions to the solar burning reaction ${}^1\text{H}(p, e^+ \nu_e){}^2\text{H}$ have later been recalculated on the basis of χEFT , and have been found to enhance the cross section obtained with single-nucleon currents by $\sim 4\%$ [34]—however, see below for a more recent assessment. Finally, parameter free calculations of the cross section for this reaction and the associated ${}^3\text{He}(p, e^+ \nu_e){}^4\text{He}$ reaction have been carried out in Ref. [35].

2.4. Nuclear charge form factors

The phenomenological success of the exchange current operators described above was mainly due to the chiral Lagrangians for the pion-nucleon couplings. The corresponding contributions to nuclear charge operators involve terms of higher power in the momentum transfer. The observation by Kloet and Tjon that there is a significant pion exchange contribution to the charge form factors of the trinucleons therefore came as a surprise [36]. This pion exchange operator brings the first diffraction minimum to lower values of momentum transfer and therefore closer to the experimental data. This observation was subsequently confirmed by a calculation of the charge form factor of the α -particle [37]. Later calculations of the charge form factors of ${}^3\text{H}$, ${}^3\text{He}$, and ${}^4\text{He}$ with realistic variational wave functions reaffirm the need for a substantial exchange charge effect for agreement with the empirical values [38]. This exchange current effect is most prominent in the lightest nuclei, and less so in the case of heavier nuclei as ${}^{16}\text{O}$ and ${}^{40}\text{Ca}$, where the shell structure is most prominent [39, 40]. The pion exchange effect nevertheless does improve slightly the agreement between the calculated and empirically extracted charge distributions throughout the periodic table [41]. The best indication of the role of the pion exchange charge operator was finally provided by the measurement of the charge form factor of the deuteron [42]. Inclusion of the exchange charge operator clearly improved the agreement with the experimental values. While the exchange charge operators that involve two nucleons were found to give substantial contributions to nuclear charge form factors, the corresponding exchange charge operators that involve three nucleons were found to give only minor contributions, because of cancellations between the pion and

rho-meson exchange operators. Those involving 4 nucleons were found to be insignificant [43].

2.5. *The axial charge operator*

That there is a significant nuclear enhancement of the axial charge of the nucleon was demonstrated by Kirchbach, Mach, and Riska, who extended the Adler-Weisberger sum rule to light nuclei [44]. A subsequent explicit calculation of the nuclear enhancement of the axial charge based on meson exchange indicated that pion-exchange mechanisms yield enhancements of the order 45–60%. In combination with short range mechanisms the total enhancement in heavy nuclei is of the order 85–100%, depending on the interaction model [45, 46]. This is sufficient to explain almost all of the empirically observed $\sim 100\%$ enhancement of first forbidden β -decay transitions in the lead region [47]. The large nuclear enhancement of the axial charge operator has later been explained within χ EFT, which provides a dynamical basis for the utility of early chiral charge algebra [48]. Finally, Lee and Riska employed the PCAC relation between the axial current and pion-production operators to show that the axial exchange current could explain the large difference between the empirical cross section for the reaction ${}^1\text{H}(p, \pi^0)pp$ and the value given by the single-nucleon pion-production operators alone [49].

2.6. *Gerry Brown and the Skyrmion*

In the late 1970's Gerry Brown engaged in a project to develop a chiral dynamics basis for quark bag models of baryons [50]. In the limit of a small bag radius this led to a connection to Skyrme's topological soliton model for the nucleon [51], which had been shown by Witten to give results that are consistent with quantum chromodynamics (QCD) in the large color limit [52]. Skyrme's topological soliton model is based on a chiral Lagrangian for pions yielding finite size solutions, which may be interpreted as baryons. The Noether currents of this Lagrangian can be viewed as models for the electromagnetic and axial currents of nucleons and nuclei. When the meson field is described by the common product ansatz for the two-nucleon system, the current operators separate into single nucleon and exchange current operators. Indeed, Nyman and Riska [25, 53] showed that if the chiral profile of the Skyrmion field for a nucleon is fitted to its electric form factor, then the deuteron form factors can be calculated with good qualitative agreement with data. In the case of the magnetic form factor

the exchange current contribution is large, and essential for agreement with the empirical form factor at large values of moment transfer. In the long-range limit there is a simple relation between the isoscalar exchange current and the phenomenological exchange current that is associated with the $\rho\pi\gamma$ vertex [26]. The long-range component of the isovector magnetic moment operator too is similar to the corresponding conventional pion-exchange magnetic-moment operator [54].

3. The chiral effective field theory approach

The last two decades have witnessed remarkable developments in nuclear χ EFT, originally proposed by Weinberg [55–57]. Chiral symmetry is an approximate symmetry of QCD, which becomes exact in the limit of vanishing quark masses. Nuclear χ EFT is the theoretical framework that permits the derivation of nuclear interactions and electroweak currents with hadronic degrees of freedom, while preserving the symmetries of QCD—the exact Lorentz, parity, and time-reversal symmetries, and the approximate chiral symmetry. The latter requires the pion couplings to hadrons to be proportional to powers of its momentum Q and, as a consequence, the Lagrangian for these interactions may be expanded in powers of Q/Λ_χ , where $\Lambda_\chi \sim 1$ GeV is the chiral symmetry breaking scale. The Lagrangians may be ordered into classes defined by the power of Q/Λ_χ , or equivalently by order of the gradients of the pion field and/or pion mass factors. Each of these contain a certain number of parameters or “low-energy constants” (LECs), which in practice are fixed by comparison with experimental data. These LECs could in principle be calculated from the underlying QCD theory of quarks and gluons, but the non-perturbative nature of the theory at low energies makes this task extremely difficult. Thus, nuclear χ EFT provides a direct connection between QCD and the strong and electroweak interactions in nuclei, and at the same time a practical calculational scheme which, at least in principle, may be improved systematically. In this sense it provides a fundamental basis for low-energy nuclear physics.

The nuclear χ EFT approach has been applied in a number of studies to derive the two- and three-nucleon potentials [58–66] including isospin-symmetry-breaking corrections [67–70]. In the electroweak sector there have been derivations of parity-violating two-nucleon potentials induced by hadronic weak interactions [71–74], constructions of nuclear electroweak currents [48], and studies of Compton scattering on nucleons and nuclei with the explicit inclusion of Δ -resonance degrees of freedom [75, 76]. Here

the focus is on nuclear electroweak current operators. These were originally derived up to one loop level in the heavy-baryon formulation of covariant perturbation theory by Park *et al.* [35, 48, 77]. More recently two independent derivations, based on time-ordered perturbation theory (TOPT), have been published—one by the present authors (RS) [78–81] and the other by Kölling *et al.* [82, 83], although these latter works only deal with electromagnetic currents. In the following, we outline the derivation of these electroweak operators, referring to the original papers [78–81] for the more technical aspects.

3.0.1. Interaction Hamiltonians

In the simplest implementation, χ EFT Lagrangians are constructed in terms of nucleon and pion degrees of freedom. This has been described in a number of papers [84, 85], and $\pi\pi$ and πN Lagrangians, denoted respectively as $\mathcal{L}_{\pi\pi}^{(m)}$ and $\mathcal{L}_{\pi N}^{(n)}$, have been derived up to high order in the chiral expansion. Contributions that arise from additional degrees of freedom, such as Δ -resonances and heavier mesons, are subsumed in the LECs of $\mathcal{L}_{\pi N}^{(n)}$ and $\mathcal{L}_{\pi\pi}^{(m)}$. In principle these Lagrangians contain an infinite number of interactions compatible with the QCD symmetries, but as the transition amplitudes obtained from them may be expanded in powers of Q/Λ_χ , the number of terms that contribute to the amplitude at any given order of the expansion is finite [55–57]. The Hamiltonians are constructed from the chiral Lagrangians by the canonical formalism.

The leading interaction terms in $\mathcal{L}_{\pi N}^{(1)}$, $\mathcal{L}_{\pi N}^{(2)}$, and $\mathcal{L}_{\pi N}^{(3)}$ in the πN sector, and $\mathcal{L}_{\pi\pi}^{(2)}$ and $\mathcal{L}_{\pi\pi}^{(4)}$ in the $\pi\pi$ sector, which are relevant to the derivation of nuclear potentials and electroweak operators at one loop level lead to the following Hamiltonians:

$$H_{\pi N} = \int d\mathbf{x} N^\dagger \left[\frac{g_A}{2f_\pi} \boldsymbol{\tau}_a \boldsymbol{\sigma} \cdot \nabla \pi_a + \frac{1}{4f_\pi^2} \boldsymbol{\tau} \cdot (\boldsymbol{\pi} \times \boldsymbol{\Pi}) + \dots \right] N, \quad (1)$$

$$H_{\gamma N} = e \int d\mathbf{x} N^\dagger \left[e_N V^0 + i \frac{e_N}{2m} \left(-\overleftarrow{\nabla} \cdot \mathbf{V} + \mathbf{V} \cdot \overrightarrow{\nabla} \right) - \frac{\mu_N}{2m} \boldsymbol{\sigma} \cdot \nabla \times \mathbf{V} \right. \\ \left. - \frac{2\mu_N - e_N}{8m^2} \left(\nabla^2 V^0 + \boldsymbol{\sigma} \times \nabla V^0 \cdot \overrightarrow{\nabla} - \overleftarrow{\nabla} \cdot \boldsymbol{\sigma} \times \nabla V^0 \right) + \dots \right] N, \quad (2)$$

$$H_{\gamma\pi} = e \int d\mathbf{x} \left[V^0 (\boldsymbol{\pi} \times \boldsymbol{\Pi})_z + \epsilon_{zab} \pi_a (\nabla \pi_b) \cdot \mathbf{V} + \dots \right], \quad (3)$$

$$H_{\gamma\pi N} = \frac{e}{2f_\pi} \int d\mathbf{x} N^\dagger \left[\frac{g_A}{2m} (\boldsymbol{\tau} \cdot \boldsymbol{\pi} + \pi_z) \boldsymbol{\sigma} \cdot \nabla V^0 - [8d_8 \nabla \pi_z \right. \\ \left. + 8d_9 \tau_a \nabla \pi_a - (2d_{21} - d_{22}) \epsilon_{zab} \tau_b \boldsymbol{\sigma} \times \nabla \pi_a] \cdot \nabla \times \mathbf{V} + \dots \right] N, \quad (4)$$

$$H_{AN} = \frac{g_A}{2} \int d\mathbf{x} N^\dagger (\tau_a \boldsymbol{\sigma} \cdot \mathbf{A}_a + \dots) N, \quad (5)$$

$$H_{A\pi} = f_\pi \int d\mathbf{x} (\mathbf{A}_a \cdot \nabla \pi_a + A_a^0 \Pi_a + \dots), \quad (6)$$

$$H_{A\pi N} = \int d\mathbf{x} N^\dagger \left[-\frac{1}{4f_\pi} A_a^0 (\boldsymbol{\tau} \times \boldsymbol{\pi})_a + \frac{2c_3}{f_\pi} \mathbf{A}_a \cdot \nabla \pi_a - \frac{c_4}{f_\pi} \epsilon_{abc} \tau_a (\mathbf{A}_b \times \nabla \pi_c) \cdot \boldsymbol{\sigma} - \frac{c_6}{4mf_\pi} (\boldsymbol{\tau} \times \boldsymbol{\pi})_a (\nabla \times \mathbf{A}_a) \cdot \boldsymbol{\sigma} + \dots \right] N, \quad (7)$$

where g_A , f_π , e , and m are, respectively, the nucleon axial coupling constant, pion decay amplitude, proton electric charge, and nucleon mass, and the parameters c_i and d_i are LECs in the $\mathcal{L}_{\pi N}^{(2)}$ and $\mathcal{L}_{\pi N}^{(3)}$ Lagrangians.

The isospin doublet of (non-relativistic) nucleon fields, isospin triplet of pion fields and conjugate fields, electromagnetic vector field and weak axial field are denoted by N , $\boldsymbol{\pi}$ and $\mathbf{\Pi}$, V^μ , and A^μ respectively, and $\boldsymbol{\sigma}$ and $\boldsymbol{\tau}$ are spin and isospin Pauli matrices. The arrow over the gradient specifies whether it acts on the left or right nucleon field. The isospin operators e_N and μ_N are defined as

$$e_N = (1 + \tau_z)/2, \quad \kappa_N = (\kappa_S + \kappa_V \tau_z)/2, \quad \mu_N = e_N + \kappa_N, \quad (8)$$

where κ_S and κ_V are the isoscalar and isovector combinations of the anomalous magnetic moments of the proton and neutron. The power counting of the resulting vertices follows by noting that each gradient brings in a factor of Q , so, for example, the two terms in $H_{\pi N}$ are both of order Q , while (ignoring the counting Q assumed for the external fields V^μ and A^μ) the first term in $H_{\gamma\pi N}$ ($H_{A\pi N}$) is of order Q (Q^0), while the remaining ones are of order Q^2 (Q^1).

In addition to the chiral Hamiltonians above, up to and including order Q^2 there are fourteen contact interaction terms allowed by the symmetries of the strong interactions, each one multiplied by a LEC. Two of these contact terms (proportional to the LECs C_S and C_T in standard notation) are of a non-derivative type, and therefore are of order Q^0 , while the remaining twelve (proportional to the LECs C'_i) of order Q^2 involve two gradients acting on the nucleon fields (these are listed in Ref. [86]). The contact potential at order Q^2 , derived from them in the two-nucleon center-of-mass system, in fact depends on C_S and C_T , and seven linear combinations of the C'_i , which are customarily denoted as C_1, \dots, C_7 . The remaining five linear combinations of C'_i have been shown to be related to C_S and C_T by requiring that the Poincaré covariance of the theory be satisfied to order Q^2 [86]. The Q^2 potential therefore involves nine independent LECs. (As

a side remark, the contact potential at order Q^4 requires an additional fifteen independent LECs.) These LECs are determined by fits to two-nucleon elastic scattering data.

Minimal substitution in the gradient terms leads to a (two-nucleon) electromagnetic contact current denoted as $\mathbf{j}_{\gamma,\text{min}}^{(1)}$ in Refs. [78, 80], where the superscript (n) specifies the power counting Q^n . Non-minimal couplings through the electromagnetic field tensor $F_{\mu\nu}$ are also allowed. It may be shown [78] that only two independent operator structures enter at order Q^1 , which lead to the contact term given by

$$\mathbf{j}_{\gamma,\text{nm}}^{(1)} = -ie \left[C'_{15} \boldsymbol{\sigma}_1 + C'_{16} \times (\tau_{1,z} - \tau_{2,z}) \boldsymbol{\sigma}_1 \right] \times \mathbf{q} + (1 \rightleftharpoons 2) \quad (9)$$

where \mathbf{q} is the external field momentum, and the isoscalar C'_{15} and isovector C'_{16} LECs (as well as the d_i 's multiplying the higher order terms in the $\gamma\pi N$ Hamiltonian) can be determined by fitting photo-nuclear data in the few-nucleon systems [80].

In the weak axial sector, there is a single contact term at order Q^0 ,

$$\mathbf{j}_{5,a}^{(0)} = z_0 (\boldsymbol{\tau}_1 \times \boldsymbol{\tau}_2)_a \left[\boldsymbol{\sigma}_1 \times \boldsymbol{\sigma}_2 - \frac{\mathbf{q}}{q^2 + m_\pi^2} \mathbf{q} \cdot (\boldsymbol{\sigma}_1 \times \boldsymbol{\sigma}_2) \right] \quad (10)$$

(here the second term of Eq. (10) is the pion-pole contribution), and none at order Q^1 . This term is due to an interaction of the type $(\bar{N}\gamma^\mu\gamma_5 N) (\bar{N}u_\mu N)$ and, as first pointed out in Ref. [87], the LEC z_0 is related to the LEC c_D (in standard notation), which enters the three-nucleon potential at leading order. The two LECs c_D and c_E which fully characterize this potential have recently been constrained by reproducing the empirical value of the Gamow-Teller matrix element in tritium β decay and the binding energies of the trinucleons [88, 89] (see below). Lastly, in the limit of small momentum transfers, there are two independent two-nucleon contact terms in the axial charge at order Q^1 [81]:

$$\begin{aligned} \rho_{5,a}^{(1)} = & i z_1 (\boldsymbol{\tau}_1 \times \boldsymbol{\tau}_2)_a (\boldsymbol{\sigma}_1 \cdot \mathbf{k}_1 - \boldsymbol{\sigma}_2 \cdot \mathbf{k}_2) \\ & + i z_2 (\boldsymbol{\sigma}_1 \times \boldsymbol{\sigma}_2) \cdot (\tau_{1,a} \mathbf{k}_2 - \tau_{2,a} \mathbf{k}_1) . \end{aligned} \quad (11)$$

The LECs z_1 and z_2 have, however yet to be determined.

3.0.2. From amplitudes to potentials and currents

Application of χ EFT to nuclear structure and bound states requires going beyond perturbation theory. As suggested by Weinberg [55–57], the formalism briefly described below for constructing nuclear potentials and currents is based on time-ordered perturbation theory (TOPT) although it

differs from Weinberg's in the way reducible contributions are dealt with. This has been employed in Refs. [78–81, 90] for constructing nuclear potentials and currents.

The terms in the TOPT expansion are conveniently represented by diagrams. Here a distinction is made between reducible diagrams, which involve at least one pure nucleonic intermediate state, and irreducible diagrams, which include pionic and nucleonic intermediate states. The contributions of the former are enhanced with respect to those of corresponding irreducible ones by a factor of Q for each pure nucleonic intermediate state. In the static limit, in which $m \rightarrow \infty$ or, equivalently, nucleon kinetic energy terms are dropped, the reducible contributions are infrared-divergent. The prescription proposed by Weinberg [55–57] to treat these is to define the nuclear potential (and currents) as given by the irreducible contributions only. The reducible contributions are generated by solution of the Lippmann-Schwinger (or Schrödinger) equation iteratively, with the nuclear potential (and currents) given by the irreducible amplitudes.

The formalism originally developed in Ref. [90] is based on this approach. The omission of the reducible contributions from the definition of the interaction operators requires care, when the irreducible amplitudes are evaluated in the static approximation, which is commonly used. The iterative process will in that limit generate only part of the reducible amplitude. The reducible part of the amplitude beyond the static approximation has then to be incorporated order by order—along with the irreducible amplitude—in the definition of nuclear operators. This scheme in combination with TOPT, which is best suited to separate the reducible content from the irreducible one, has been implemented in Refs. [78–81] and is described below. The method does however lead to nuclear operators, which are not uniquely defined because of the non-uniqueness of the transition amplitude off-the-energy shell. This lack of uniqueness is immaterial, however, because the resulting operators are unitarily equivalent, and therefore the description of physical observables is not affected by this ambiguity [79].

Another approach for overcoming the difficulties posed by the reducible amplitudes, has been introduced by Epelbaum and collaborators [59]. That method is usually referred to as the unitary transformation method and is based on TOPT. It exploits the Okubo (unitary) transformation [91] to decouple the Fock space of pions and nucleons into two subspaces, one that has pure nucleonic states and the other with states which retain at least one pion. In this decoupled space, the amplitude does not involve enhanced

contributions associated with the reducible diagrams. The subspaces are not uniquely defined, as it is always possible to perform additional unitary transformations on them, with a consequent change in the formal definition of the resulting nuclear operators. This, of course, does not affect the calculated physical observables.

The two TOPT-based methods outlined above lead to formally equivalent operator structures for the nuclear potential and electromagnetic currents up to loop-corrections included [80]. It is natural to conjecture that the two methods are closely related, although this remains to be proved. Below we briefly outline the methods developed in Refs. [78–81] and sketch how nuclear operators are derived from transition amplitudes.

We start from the conventional perturbative expansion of the NN scattering amplitude T :

$$\langle f | T | i \rangle = \langle f | H_1 \sum_{n=1}^{\infty} \left(\frac{1}{E_i - H_0 + i\eta} H_1 \right)^{n-1} | i \rangle. \quad (12)$$

Here $|i\rangle$ and $|f\rangle$ represent the initial and final NN states with energy $E_i = E_f$, H_0 is the Hamiltonian describing free pions and nucleons, and H_1 is the Hamiltonian describing interactions between them (see Sec. 3.0.1). The evaluation of this amplitude is in practice carried out by inserting complete sets of H_0 eigenstates between successive terms of H_1 . Power counting is then used to organize the expansion.

In the perturbation expansion of Eq. (12), a generic (reducible or irreducible) contribution is characterized by a certain number, say M , of vertices, each scaling as $Q^{\alpha_i} \times Q^{-\beta_i/2}$ ($i=1, \dots, M$), where α_i is the power counting implied by the relevant interaction Hamiltonian and β_i is the number of pions in and/or out of the vertex, a corresponding $M - 1$ number of energy denominators, and possibly L loops. Out of these $M - 1$ energy denominators, M_K will involve only nucleon kinetic energies, which scale as Q^2 , and the remaining $M - M_K - 1$ will involve, in addition, pion energies, which are of order Q . Loops, on the other hand, contribute a factor Q^3 each, since they imply integrations over intermediate three momenta. Hence the power counting associated with such a contribution is

$$\left(\prod_{i=1}^M Q^{\alpha_i - \beta_i/2} \right) \times \left[Q^{-(M - M_K - 1)} Q^{-2M_K} \right] \times Q^{3L}. \quad (13)$$

Clearly, each of the $M - M_K - 1$ energy denominators can be further expanded as

$$\frac{1}{E_i - E_I - \omega_\pi} = -\frac{1}{\omega_\pi} \left[1 + \frac{E_i - E_I}{\omega_\pi} + \frac{(E_i - E_I)^2}{\omega_\pi^2} + \dots \right], \quad (14)$$

where E_I denotes the kinetic energy of the intermediate two-nucleon state, ω_π the pion energy (or energies, as the case may be), and the ratio $(E_i - E_I)/\omega_\pi$ is of order Q . The terms proportional to powers of $(E_i - E_I)/\omega_\pi$ lead to non-static corrections.

The Q -scaling of the interaction vertices and the considerations above show that the amplitude T admits the following expansion:

$$T = T^{(\nu)} + T^{(\nu+1)} + T^{(\nu+2)} + \dots, \quad (15)$$

where $T^{(n)} \sim Q^n$, and chiral symmetry ensures that ν is finite. In the case of the two-nucleon potential $\nu = 0$. A two-nucleon potential v can then be derived, which when iterated in the Lippmann-Schwinger (LS) equation,

$$v + v G_0 v + v G_0 v G_0 v + \dots, \quad (16)$$

leads to the on-the-energy-shell ($E_i = E_f$) T -matrix in Eq. (15), order by order in the power counting. In practice, this requirement can only be satisfied up to a given order n^* , and the resulting potential, when inserted into the LS equation, will generate contributions of order $n > n^*$, which do not match $T^{(n)}$. In Eq. (16), G_0 denotes the free two-nucleon propagator, $G_0 = 1/(E_i - E_I + i\eta)$, and we assume that

$$v = v^{(0)} + v^{(1)} + v^{(2)} + \dots, \quad (17)$$

where the still to be determined term $v^{(n)}$ is of order Q^n . We also note that, generally, a term like $v^{(m)} G_0 v^{(n)}$ is of order Q^{m+n+1} , since G_0 is of order Q^{-2} and the implicit loop integration brings in a factor Q^3 .

Having established the above power counting, we obtain

$$v^{(0)} = T^{(0)}, \quad (18)$$

$$v^{(1)} = T^{(1)} - \left[v^{(0)} G_0 v^{(0)} \right], \quad (19)$$

$$v^{(2)} = T^{(2)} - \left[v^{(0)} G_0 v^{(0)} G_0 v^{(0)} \right] - \left[v^{(1)} G_0 v^{(0)} + v^{(0)} G_0 v^{(1)} \right]. \quad (20)$$

The leading-order (LO) Q^0 term, $v^{(0)}$, consists of (static) one-pion exchange (OPE) and two (non-derivative) contact interactions, while the next-to-leading (NLO) Q^1 term, $v^{(1)}$, is easily seen to vanish [79], since the leading non-static corrections $T^{(1)}$ to the (static) OPE amplitude add up to zero on the energy shell, while the remaining diagrams in $T^{(1)}$ represent iterations of $v^{(0)}$, whose contributions are exactly canceled by $[v^{(0)} G_0 v^{(0)}]$ (complete or partial cancellations of this type persist at higher $n \geq 2$ orders). The

next-to-next-to-leading (N2LO) Q^2 term, which follows from Eq. (20), contains two-pion-exchange (TPE) and contact (involving two gradients of the nucleon fields) interactions.

The inclusion (in first order) of electroweak interactions in the perturbative expansion of Eq. (12) is in principle straightforward. The transition operator can be expanded as [79, 81]:

$$T_{\text{ext}} = T_{\text{ext}}^{(\nu_e)} + T_{\text{ext}}^{(\nu_e+1)} + T_{\text{ext}}^{(\nu_e+2)} + \dots, \quad (21)$$

where $T_{\text{ext}}^{(n)}$ is of order Q^n and $\nu_e = -3$ in this case. The nuclear electromagnetic (weak axial) charge, ρ_γ ($\rho_{5,a}$), and current, \mathbf{j}_γ ($\mathbf{j}_{5,a}$), operators follow from $v_\gamma = V^0 \rho_\gamma - \mathbf{V} \cdot \mathbf{j}_\gamma$ ($v_5 = A_a^0 \rho_{5,a} - \mathbf{A}_a \cdot \mathbf{j}_{5,a}$), where $V^\mu = (V^0, \mathbf{V})$ [$A_a^\mu = (A_a^0, \mathbf{A}_a)$] is the electromagnetic vector (weak axial) field, and it is assumed that v_{ext} has a similar expansion as T_{ext} . The requirement that, in the context of the LS equation, v_{ext} matches T_{ext} order by order in the power counting implies relations for the $v_\gamma^{(n)} = V^0 \rho_\gamma^{(n)} - \mathbf{V} \cdot \mathbf{j}_\gamma^{(n)}$ and $v_5^{(n)} = A_a^0 \rho_{5,a}^{(n)} - \mathbf{A}_a \cdot \mathbf{j}_{5,a}^{(n)}$, which can be found in Refs. [79, 81], similar to those derived above for $v^{(n)}$, the strong-interaction potential.

The lowest order terms that contribute to the electromagnetic charge and axial current operators have $\nu_e = -3$,

$$\rho_\gamma^{(-3)} = e \frac{1 + \tau_{1,z}}{2} + (1 \Rightarrow 2), \quad (22)$$

$$\mathbf{j}_{5,a}^{(-3)} = -\frac{gA}{2} \tau_{1,a} \left(\boldsymbol{\sigma}_1 - \frac{\mathbf{q}}{q^2 + m_\pi^2} \boldsymbol{\sigma}_1 \cdot \mathbf{q} \right) + (1 \Rightarrow 2). \quad (23)$$

There are no Q^{-3} contributions to \mathbf{j} and $\rho_{5,a}$, and the lowest order ($\nu_e = -2$) consists of electromagnetic current and axial charge operators, given by

$$\mathbf{j}_\gamma^{(-2)} = \frac{e}{2m} \left(2 \mathbf{K}_1 \frac{1 + \tau_{1,z}}{2} + i \boldsymbol{\sigma}_1 \times \mathbf{q} \frac{\mu^S + \mu^V \tau_{1,z}}{2} \right) + (1 \Rightarrow 2), \quad (24)$$

$$\rho_{5,a}^{(-2)} = -\frac{gA}{2m} \tau_{1,a} \boldsymbol{\sigma}_1 \cdot \mathbf{K}_1 + (1 \Rightarrow 2), \quad (25)$$

where \mathbf{k}_i and \mathbf{K}_i denote hereafter the combinations of initial and final nucleon momenta

$$\mathbf{k}_i = \mathbf{p}'_i - \mathbf{p}_i, \quad \mathbf{K}_i = (\mathbf{p}'_i + \mathbf{p}_i)/2. \quad (26)$$

The counting Q^{-3} (Q^{-2}) in the electromagnetic charge and axial current (electromagnetic current and axial charge) operators follows from the product of the power counting associated with the γNN , ANN , $A\pi$, and πNN vertices, and the Q^{-3} factor due to the momentum-conserving δ -function implicit in disconnected terms of this type.

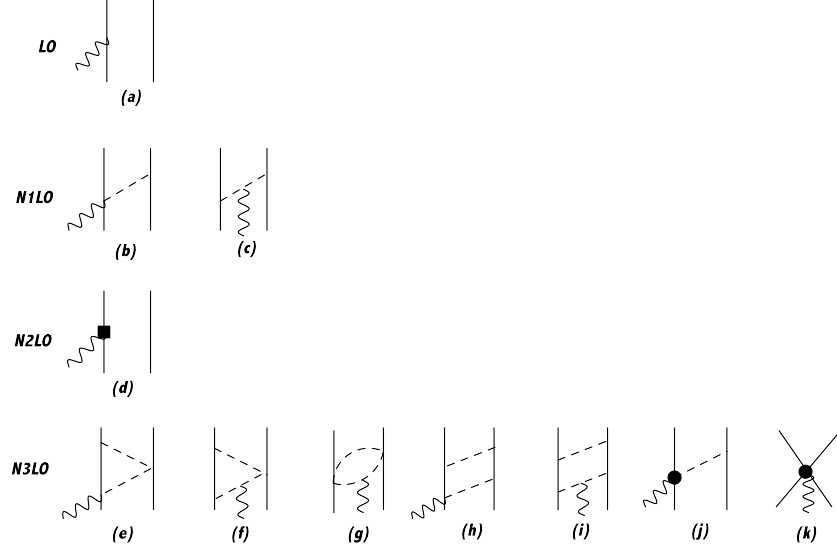


Fig. 1. Diagrams illustrating one- and two-body electromagnetic currents entering at Q^{-2} (LO), Q^{-1} (NLO), Q^0 (N2LO), and Q^1 (N3LO). Nucleons, pions, and photons are denoted by solid, dashed, and wavy lines, respectively. The square in panel (d) represents the $(Q/m)^2$ relativistic correction to the LO one-body current; the solid circle in panel (j) is associated with the $\gamma\pi N$ current coupling of order Q , involving the LECs d_8 , d_9 , and $2d_{21} - d_{22}$; the solid circle in panel (k) denotes two-body contact terms of minimal and non-minimal nature, the latter involving the LECs C'_{15} and C'_{16} . Only one among all possible time orderings is shown for the NLO and N3LO currents, so that all direct- and crossed-box contributions are accounted for.

The contributions up to one loop to the electromagnetic current and charge operators are illustrated diagrammatically in Figs. 1 and 2, while those to the weak axial current and charge operators in Figs. 3 and 4. As already noted, the LO starts at $\nu_e = -2$ for the electromagnetic current and axial charge and at $\nu_e = -3$ for the electromagnetic charge and axial current; n NLO corrections to these are labelled as $Q^n \times \text{LO}$. We begin by discussing the electromagnetic operators.

The electromagnetic currents from LO, NLO, and N2LO terms and from N3LO loop corrections depend only on the known parameters g_A and f_π (NLO and N3LO), and the nucleon magnetic moments (LO and N2LO). Unknown LECs enter the N3LO OPE contribution involving the $\gamma\pi N$ vertex of order Q^2 from $H_{\gamma\pi N}$, the term proportional to the d_i in Eq. (4),

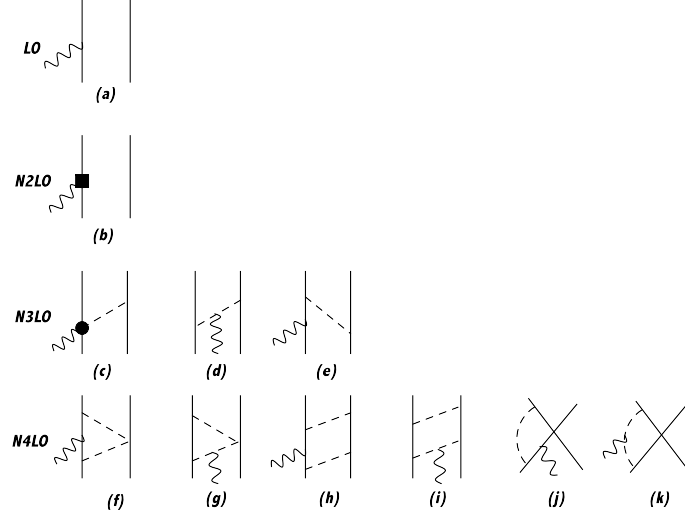


Fig. 2. Diagrams illustrating one- and two-body electromagnetic charge operators entering at Q^{-3} (LO), Q^{-1} (N2LO), Q^0 (N3LO), Q^1 (N4LO). The square in panel (b) represents the $(Q/m)^2$ relativistic correction to the LO one-body charge operator, whereas the solid circle in panel (c) is associated with a $\gamma\pi N$ charge coupling of order Q . As in Fig. 1, only a single time ordering is shown for the N3LO and N4LO charge operators.

as well as the contact currents implied by non-minimal couplings, Eq. (9), discussed in the next subsection. On the other hand, in the charge operator there are no unknown LECs up to one loop level, and OPE contributions, illustrated in panels (c)-(e) of Fig. 2, only appear at N3LO. The contributions in panels (d) and (e) involve non-static corrections [79], while the contribution in panel (c) is associated with the $\gamma\pi N$ coupling of order Q originating from the first term in Eq. (4). It leads to a two-body charge operator:

$$\rho_\gamma^{(0)}(\text{OPE}) = \frac{e}{8m} \frac{g_A^2}{f_\pi^2} (\boldsymbol{\tau}_1 \cdot \boldsymbol{\tau}_2 + \tau_{2z}) \frac{\boldsymbol{\sigma}_1 \cdot \mathbf{q} \boldsymbol{\sigma}_2 \cdot \mathbf{k}_2}{k_2^2 + m_\pi^2} + (1 \rightleftharpoons 2). \quad (27)$$

In the present χ EFT context, $\rho_\pi^{(0)}$ was derived first by Phillips in 2003 [92]. However, the operator of Eq. (27) is the same as the π -exchange contribution derived within the conventional approach (see Ref. [93] and references therein). This operator plays an important role in yielding predictions for the $A=2-4$ charge form factors that are in very good agreement with the experimental data at low and moderate values of the momentum transfer

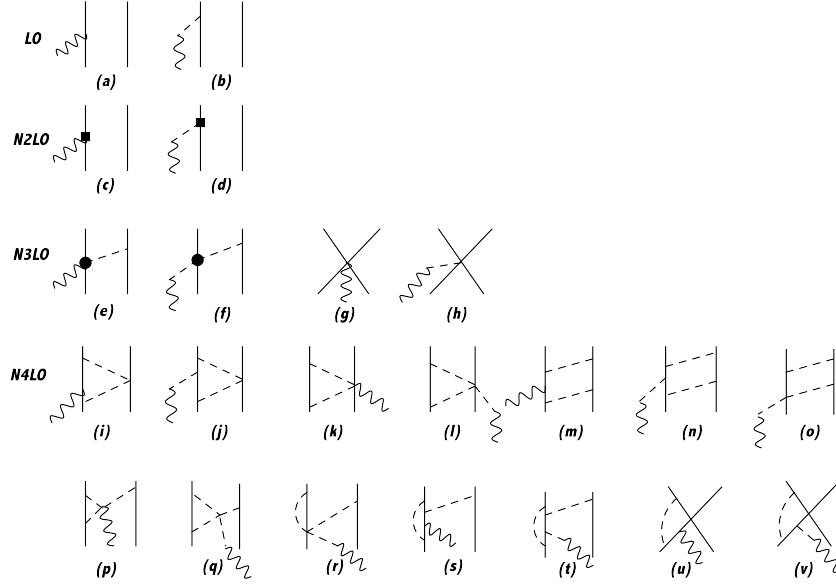


Fig. 3. Diagrams illustrating one- and two-body axial currents entering at Q^{-3} (LO), Q^{-1} (N2LO), Q^0 (N3LO), and Q^1 (N4LO). Nucleons, pions, and axial fields are denoted by solid, dashed, and wavy lines, respectively. The squares in panels (c) and (d) denote relativistic corrections to the one-body axial current, while the circles in panels (e) and (f) represent vertices implied by the $\mathcal{L}_{\pi N}^{(2)}$ chiral Lagrangian, involving the LECs c_i (see Ref. [81] for additional explanations). As in Fig. 1, only a single time ordering is shown.

($q \lesssim 5 \text{ fm}^{-1}$) [80, 94]. The calculations in Ref. [80] also showed that the OPE contributions from panels (d) and (e) of Fig. 2 are typically an order of magnitude smaller than those generated by panel (c).

The axial current and charge operators illustrated in Figs. 3 and 4 include pion-pole contributions, which are crucial for the current to be conserved in the chiral limit [81] (these contributions were ignored in the earlier studies of Park *et al.* [35, 48]; obviously, they are suppressed in low momentum transfer processes). It is also interesting to note that there are no direct couplings of A_a^0 to the nucleon, see panel (a) in Fig. 4. In the axial current pion-range contributions enter at N3LO, panels (e) and (f) of Fig. 3, and involve vertices from the sub-leading $\mathcal{L}_{\pi N}^{(2)}$ Lagrangian, proportional to the LECs c_3 , c_4 , and c_6 . It is given by (the complete operator, including

pion pole contributions, is listed in Ref. [81])

$$\mathbf{j}_{5,a}^{(0)}(\text{OPE}) = \frac{g_A}{2f_\pi^2} \left\{ 2c_3 \tau_{2,a} \mathbf{k}_2 + (\boldsymbol{\tau}_1 \times \boldsymbol{\tau}_2)_a \left[\frac{i}{2m} \mathbf{K}_1 - \frac{c_6 + 1}{4m} \boldsymbol{\sigma}_1 \times \mathbf{q} + \left(c_4 + \frac{1}{4m} \right) \boldsymbol{\sigma}_1 \times \mathbf{k}_2 \right] \right\} \frac{\boldsymbol{\sigma}_2 \cdot \mathbf{k}_2}{k_2^2 + m_\pi^2} + (1 \rightleftharpoons 2). \quad (28)$$

In contrast, the axial charge has a OPE contribution at NLO, illustrated in panels (b) and (c) of Fig. 4, which reads

$$\rho_{5,a}^{(-1)}(\text{OPE}) = i \frac{g_A}{4f_\pi^2} (\boldsymbol{\tau}_1 \times \boldsymbol{\tau}_2)_a \frac{\boldsymbol{\sigma}_2 \cdot \mathbf{k}_2}{k_2^2 + m_\pi^2} + (1 \rightleftharpoons 2). \quad (29)$$

In fact, an operator of precisely this form was derived by Kubodera *et al.* [95] in the late seventies, long before the systematic approach based on chiral Lagrangians now in use was established. Corrections to the axial current at N4LO in panels (i)-(v) of Fig. 3 and those to the axial charge at N3LO in panels (d)-(n) of Fig. 4 have yet to be included in actual calculations of weak transitions in nuclei. It is worthwhile noting that vertices involving three or four pions, such as those, for example, occurring in panels (l), (p), (q) and (r) of Fig. 3, depend on the pion field parametrization. This dependence must cancel out after summing the individual contributions associated with these diagrams, as indeed it does [81] (this and the requirement, remarked on below, that the axial current be conserved in the chiral limit provide useful checks of the calculation).

The loop integrals in the diagrams of Figs. 1–4 are ultraviolet divergent and are regularized in dimensional regularization [78, 79, 81–83]. In the electromagnetic current the divergent parts of these loop integrals are reabsorbed by the LECs C'_i [78, 83], while those in the electromagnetic charge cancel out, in line with fact that there are no counter-terms at N4LO [79, 83]. In the case of the axial operators [48, 81], there are no divergencies in the current, while those in the charge lead to renormalization of the LECs multiplying contact-type contributions. In particular, the infinities in loop corrections to the OPE axial charge (not shown in Fig. 4) are re-absorbed by renormalization of the LECs d_i in the $\mathcal{L}_{\pi N}^{(3)}$ Lagrangian. For a discussion of these issues we defer to Ref. [81].

We conclude this subsection by pointing out that at the present time two-nucleon potentials have been derived, and widely used, up to order $(Q/\Lambda_\chi)^4$ (or $v^{(4)}$, requiring two-loop contributions). Very recently, a new derivation up to order $(Q/\Lambda_\chi)^5$ has appeared [96]. Some of these high-order potentials have been used, in conjunction with the one-loop operators presented here, in calculations of electroweak observables of light nuclei, as reported below. Conservation of the electromagnetic current $\mathbf{q} \cdot \mathbf{j}_\gamma = [H, \rho_\gamma]$

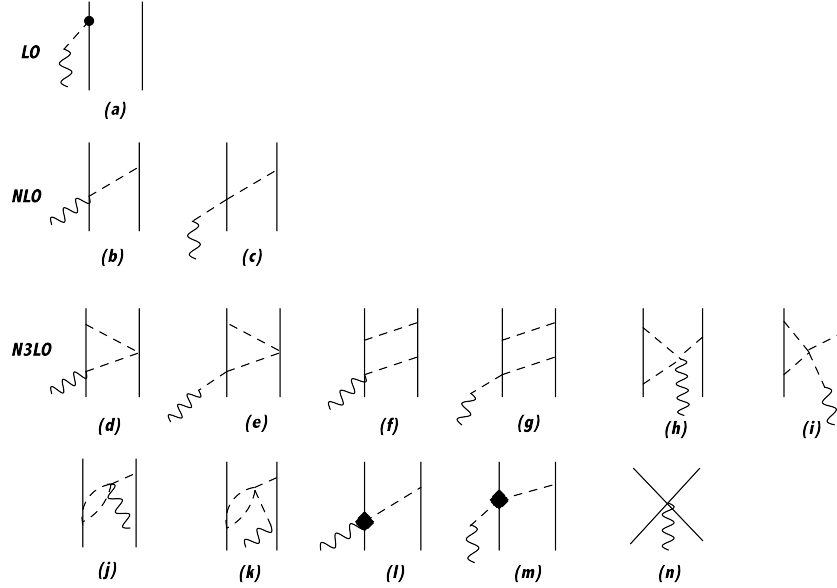


Fig. 4. Diagrams illustrating one- and two-body axial charge operators entering at Q^{-2} (LO), Q^{-1} (NLO), and Q^1 (N3LO). Nucleons, pions, and axial fields are denoted by solid, dashed, and wavy lines, respectively. The diamonds in panels (l) and (m) indicate higher order $A\pi N$ vertices implied by the $\mathcal{L}_{\pi N}^{(3)}$ chiral Lagrangian, involving the LECs d_i (see Ref. [81] for additional explanations). As in Fig. 1, only a single time ordering is shown.

with the two-nucleon Hamiltonian given by $H = T^{(-1)} + v^{(0)} + v^{(2)} + \dots$ and where the (two-nucleon) kinetic energy $T^{(-1)}$ is counted as Q^{-1} , implies [78], order by order in the power counting, a set of non-trivial relations between the $\mathbf{j}_\gamma^{(n)}$ and the $T^{(-1)}$, $v^{(n)}$, and $\rho_\gamma^{(n)}$ (note that commutators implicitly bring in factors of Q^3)—incidentally, similar considerations also apply to the conservation of the axial current in the chiral limit [81]. These relations couple different orders in the power counting of the operators, making it impossible to carry out a calculation, which at a given n for $\mathbf{j}_\gamma^{(n)}$, $v^{(n)}$, and $\rho_\gamma^{(n)}$ (and hence “consistent” from a power-counting perspective) also leads to a conserved current.

4. Results

In this section we provide a sample of results obtained with χ EFT electroweak currents for light systems, including $A = 2$ –4 nuclei and s - and p -shell nuclei in the mass range $A = 6$ –10, in the last five years or so. The few-nucleon calculations are based on the chiral two-nucleon potentials developed by Entem and Machleidt [60, 61] at order Q^4 in the power counting including up to two-loop corrections, and chiral three-nucleon potentials at leading order [97]. (Below, this combination of two and three-nucleon potentials will be referred to as N3LO/N2LO, as is customarily done in the literature, even though such a classification does not conform to the power-counting notation adopted in the present chapter.) As noted earlier, the two LECs c_D —related to the LEC z_0 in the contact axial current of Eq. (10)—and c_E entering the three-nucleon potential have been constrained by fitting the Gamow-Teller matrix element in tritium β -decay and the binding energies of the trinucleons [88, 89].

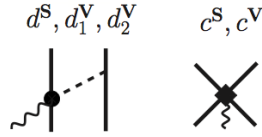


Fig. 5. The isoscalar d^S and c^S , and isovector d_1^V , d_2^V , and c^V LECs characterizing the electromagnetic current at N3LO.

The electroweak operators in Figs. 1–4 have power law behavior for large momenta, and need to be regularized before they can be sandwiched between nuclear wave functions. The regulator is taken of the form $C_\Lambda(k) = \exp[-(k/\Lambda)^n]$ with $n = 4$ and Λ in the range (500–600) MeV. For processes involving low momentum and energy transfers one would expect predictions to be fairly insensitive to variations of Λ . As shown below, this expectation is borne out in actual calculations, at least in the case of processes which are not inhibited at leading order, such as the n ^3He radiative capture or p ^3He weak fusion.

There are 5 unknown LECs in \mathbf{j} —see Fig. 5 or panels (j) and (k) of Fig. 1—and none in ρ [78, 80, 82, 83]. Two (three) of these LECs multiply isoscalar (isovector) operators. For each Λ the two isoscalar LECs are fixed by reproducing the deuteron and isoscalar trinucleon magnetic moments. Two of the isovector LECs are then constrained by assuming Δ -resonance

Table 1. Values for the LECs in units $1/\Lambda^2$ for d^S and $1/\Lambda^4$ for c^S and c^V ; see text for further explanations.

Λ MeV	c^S	$d^S \times 10$	$c^V(\sigma_{np})$	$c^V(\mu^V)$
500	4.1	2.2	-13	-8.0
600	11	3.2	-22	-12

saturation [80], while the remaining LEC is determined by reproducing (again for each Λ) either the np radiative capture cross section σ_{np} at thermal neutron energies or the isovector trinucleon magnetic moment μ^V [80]. There are no three-body currents entering at the order of interest [98], and so it is possible to use three-nucleon observables to fix some of these LECs. Their values are listed in Table 1. They are generally rather large, particularly when c^V is determined by the np radiative capture cross section. The exception is the isoscalar LEC d^S multiplying the one-pion exchange current involving a sub-subleading $\gamma\pi N$ vertex from the chiral Lagrangian $\mathcal{L}_{\pi N}^{(3)}$, which in a resonance-saturation picture reduces to the $\rho\pi\gamma$ transition current.

The calculations of $A = 6$ – 10 nuclei are carried out in the hybrid approach, in which χ EFT electroweak currents are used in combination with the Argonne v_{18} two-nucleon (AV18) and Illinois-7 three-nucleon (IL7) potentials. The AV18 consists of a long-range component induced by OPE and intermediate-to-short range components modeled phenomenologically and constrained to fit the NV database beyond the pion-production threshold ($E_{\text{lab}} = 350$ MeV). The IL7 includes a central (albeit isospin dependent) short-range repulsive term and two- and three-pion-exchange mechanisms involving excitation of intermediate Δ resonances. Its strength is determined by four parameters which are fixed by a best fit to the energies of 17 low-lying states of nuclei in the mass range $A \leq 10$, obtained in combination with the AV18 potential. The AV18/IL7 Hamiltonian then leads to predictions of ~ 100 ground- and excited-state energies up to $A = 12$, including the ^{12}C ground- and Hoyle-state energies, in good agreement with the corresponding empirical values (for a recent review of these as well as results obtained for nuclear and neutron matter, see Ref. [99]).

4.1. Electromagnetic observables of $A = 2-4$ nuclei

The deuteron magnetic form factor, calculated in Ref. [80], is shown in Fig. 6. The bands reflect the sensitivity to cutoff variations in the range $\Lambda = (500-600)$ MeV. The black bands include all corrections up to N3LO in the (isoscalar) electromagnetic (EM) current. The NLO OPE and N3LO TPE currents are isovector and therefore give no contributions to this observable. The right panel of Fig. 6 contains a comparison of the results of Ref. [80] with those of a calculation based on a lower order potential and in which a different strategy was adopted for constraining the LEC's d^S and c^S in the N3LO EM current [100]. This figure and the following Fig. 2 are from the recent review paper by S. Bacca and S. Pastore [101].

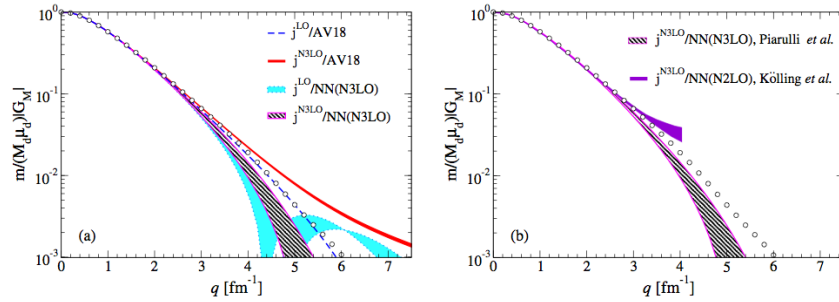


Fig. 6. Magnetic form factor of the deuteron: the left panel shows results obtained with LO and N3LO currents and either the chiral N3LO or conventional AV18 potential; the right panel shows results obtained with N3LO currents and either the chiral N3LO (same as in left panel) or a chiral N2LO potential by Kölling *et al.*. The bands reflect cutoff variation. Experimental data are the empty circles.

The predicted magnetic form factors of the ${}^3\text{He}$ and ${}^3\text{H}$ ground states are compared to experimental data in Fig. 7 [80]. Isovector OPE and TPE two-body terms in the EM current play an important role in these observables, confirming previous results obtained in the conventional meson-exchange framework. We show the N3LO results corresponding to the two different ways used to constrain the LEC c^V in the isovector contact current (recall the the LECs d_1^V and d_2^V are assumed to be saturated by the Δ resonance), namely by reproducing (i) the empirical value for the np cross section—curve labeled N3LO(σ_{np})—or (ii) the isovector magnetic moment of ${}^3\text{He}/{}^3\text{H}$ —curve labeled N3LO(μ^V). The bands display the cutoff sensitivity, which becomes rather large for momentum transfers $q \gtrsim 3 \text{ fm}^{-1}$. The N3LO(σ_{np}) results are in better agreement with the data at higher

momentum transfers; however, they overestimate μ^V by $\sim 2\%$. On the other hand, the N3LO(μ^V) results, while reproducing μ^V by construction, under-predict σ_{np} by $\sim 1\%$.

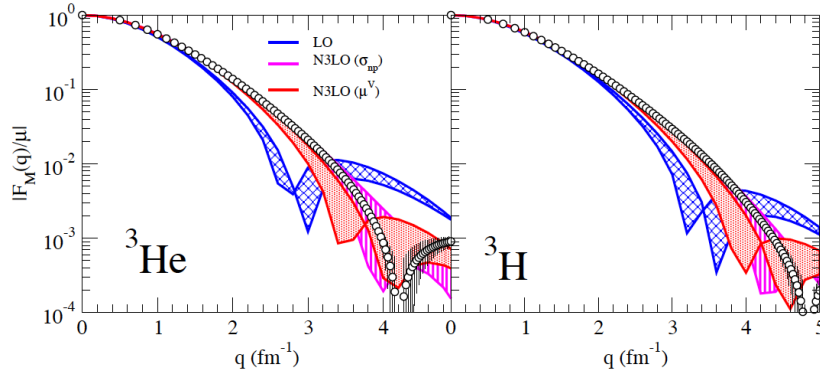


Fig. 7. Magnetic form factors of ${}^3\text{He}$ (left panel) and ${}^3\text{H}$ (right panel); see text for further explanations.

Moving on to the EM charge operator, we show in Figs. 8 and 9 very recent calculations of the deuteron monopole and quadrupole form factors [80] and ${}^4\text{He}$ (charge) form factor [102]. There are no unknown LECs beyond g_A , f_π and the nucleon magnetic moments—the latter enter a relativistic correction, suppressed by Q^2 relative to the LO charge operator, *i.e.*, the well-known spin-orbit term. The loop contributions (at N4LO) from two-pion exchange are isovector and hence vanish for these observables.

The deuteron monopole and quadrupole form factor data are obtained from measurements of the A structure function and tensor polarization observable in electron-deuteron scattering. In Fig. 8 the two bands correspond to two different calculations, one of which, labeled as NN(N2LO), is based on a lower order chiral potential [92, 103]. There is good agreement between theory and experiment. Differences between the two sets of theory predictions merely reflect differences in the deuteron wave functions obtained with the N3LO and N2LO potentials. These differences are amplified in the diffraction region of the monopole form factor.

The ${}^4\text{He}$ charge form factor is obtained from elastic electron scattering cross section data. These data now extend up to momentum transfers $q \lesssim 10 \text{ fm}^{-1}$ [104], well beyond the range of applicability of χEFT . In Fig. 9

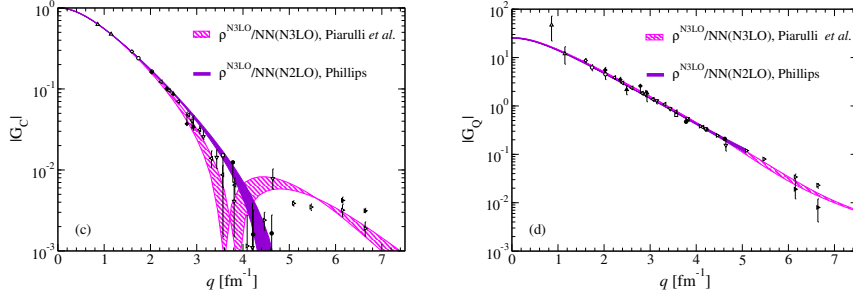


Fig. 8. The deuteron monopole and quadrupole form factors obtained from measurements of the A structure function and tensor polarization are compared to predictions based on N2LO and N3LO chiral potentials.

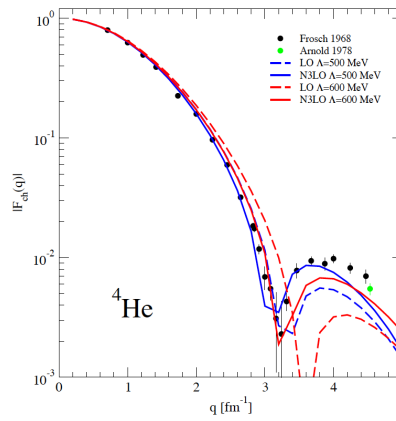


Fig. 9. The ${}^4\text{He}$ charge form factor obtained from elastic electron scattering data is compared to results obtained with the LO and N3LO charge operator.

only data up to $q \lesssim 5 \text{ fm}^{-1}$ are shown. They are in excellent agreement with theory.

Predictions for the charge radii of the deuteron and helium isotopes and for the deuteron quadrupole moment (Q_d) are listed in Table 2 [80]. They are within 1% of experimental values. It is worth noting that until recently calculations based on the conventional meson-exchange framework used to consistently underestimate Q_d . However, this situation has now changed, and a relativistic calculation in the covariant spectator theory based on a one-boson exchange model of the NN interaction has led to a value for the

Table 2. The charge radii of the ${}^2\text{H}$, ${}^3\text{He}$, and ${}^4\text{He}$ nuclei, and ${}^2\text{H}$ quadrupole moment. The numbers in parentheses at the side of the χEFT predictions give the cutoff dependence of the results.

	$r_c({}^2\text{H})$ (fm)	Q_d (fm ²)	$r_c({}^3\text{He})$ (fm)	$r_c({}^4\text{He})$ (fm)
χEFT	2.126(4)	0.2836(16)	1.962(4)	1.663(11)
EXP	2.130(10)	0.2859(6)	1.973(14)	1.681(4)

quadrupole moment [105] which is in agreement with experiment.

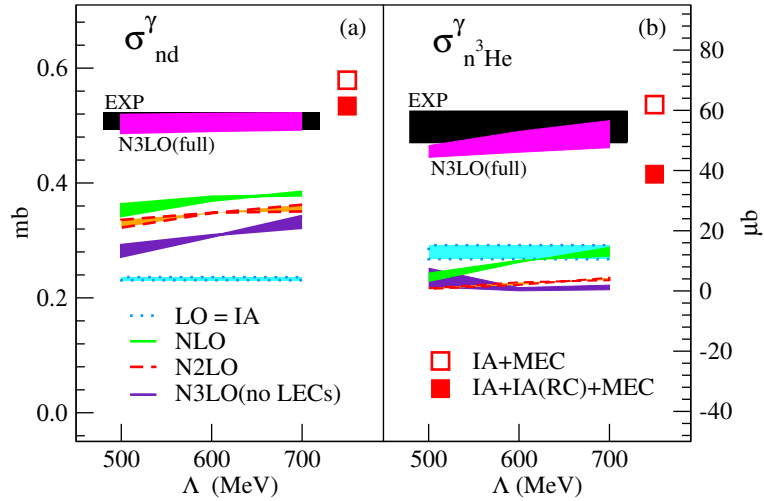


Fig. 10. Results for the nd and $n{}^3\text{He}$ radiative capture cross sections, obtained by including cumulatively the LO, NLO, N2LO, N3LO(no LECs), and N3LO(full) contributions from the χEFT electromagnetic current. Also shown are predictions obtained in the conventional approach based on the AV18/UIX Hamiltonian and accompanying effective-meson exchange currents, the square labeled IA+MEC and IA+IA(RC)+MEC, the latter including relativistic correction to the IA operator. The black band represents the experimental data, see text for further explanations.

As a last example we show in Fig. 10 predictions for the nd and $n{}^3\text{He}$ radiative capture cross sections at thermal neutron energies [98]. It is well known that these $M1$ transitions are suppressed when the magnetic dipole operator is taken to consist only of proton and neutron contributions, i.e., in the impulse approximation (IA). The results shown in Fig. 10 have been obtained from highly accurate (essentially exact) solutions of the bound

and continuum states of the $A = 3$ and 4 systems with the hyperspherical-harmonics technique [106], based on both chiral and conventional two- and three-nucleon potentials, the N3LO/N2LO and AV18/UIX, and chiral electromagnetic currents up to N3LO. However, in this earlier study, the procedure adopted to fix the three isovector LECs is different from that utilized in the calculations discussed so far. Here Δ -resonance saturation is exploited only to fix the ratio of the two LECs d_1^V and d_2^V in the tree-level contribution of Fig. 5, and the remaining two (isovector) LECs are then determined by a simultaneous fit to σ_{np} and the isovector combination of the trinucleon magnetic moment. Furthermore, the LECs in the contact current originating from minimal couplings have been taken from a lower order (NLO) chiral potential [78] rather than from the N3LO potential of Ref. [60, 61].

In Fig. 10 the experimental data are from Ref. [107] for nd and Refs. [108, 109] for $n^3\text{He}$, the band thickness denoting the error. Results obtained with the complete N3LO χEFT operator are shown by the orange band labeled N3LO(full): those corresponding to the N3LO/N2LO (AV18/UIX) model delimit the lower (upper) end of the band in the case of nd , and its upper (lower) end in the case of $n^3\text{He}$. There is considerable cutoff dependence, particularly for the four-body capture. In this connection, it is interesting to note the crucial role played by the N3LO currents in Fig. 5: indeed, retaining only the minimal contact currents and the currents from TPE loop corrections—bands labeled N3LO(no LECs)—would severely under-estimate the measured cross sections. It is clear that the convergence of the chiral expansion for these processes is problematic. The LO (or IA) is unnaturally small, since the associated operator cannot connect the dominant S-states in the hydrogen and helium bound states. This leads to an enhancement of the NLO contribution, which, however, in the case of $n^3\text{He}$, is offset by the destructive interference between it and the LO contribution. Thus a satisfactory description of these processes remains particularly challenging for nuclear theory and nuclear χEFT in particular.

4.2. *Electromagnetic transitions in $A = 6$ –10 nuclei*

Heavier systems offer new challenges and opportunities for applications of nuclear χEFT , and *ab initio* studies of electroweak processes based on this approach in systems with $A > 4$ have only just begun. In the mass range $A = 6$ –12 Variational Monte Carlo (VMC) and Green's function Monte Carlo (GFMC) methods allow us to carry out accurate, in fact exact in

the case of GFMC, first-principles calculations of many nuclear properties (see Ref [99] for a recent review). However, since these methods are formulated in configuration space, it has not been possible to use them in conjunction with the chiral two- and three-nucleon potentials above, which are given in momentum-space (and are strongly non-local in configuration space). A first step in this direction is the very recent development of a class of configuration-space, minimally non-local two-nucleon chiral potentials that fit the np and pp database up to the pion-production threshold with a χ^2 per datum close to 1.3 [110], i.e., of the same quality as the well established N³LO models of Refs. [60, 61]. Use of these potentials in VMC and, especially, GFMC calculations of light s- and p-shell nuclei will expand the scope of the nuclear χ EFT approach, and in particular test its validity beyond the realm of few-nucleon systems, to which it has primarily been limited so far.

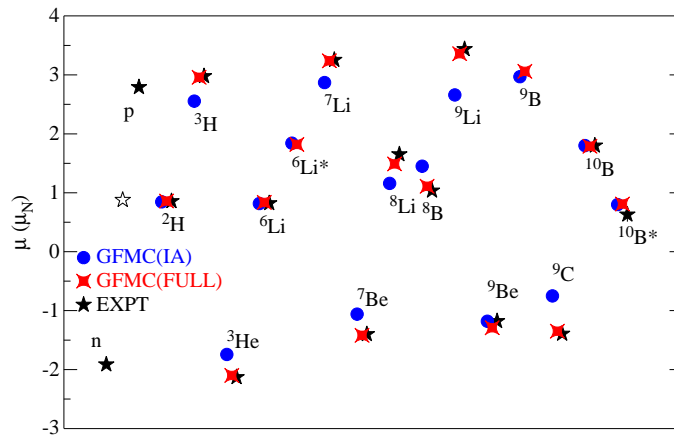


Fig. 11. Magnetic moments in nuclear magnetons for $A \leq 10$ nuclei obtained in GFMC calculations based on the conventional AV18/IL7 Hamiltonian and chiral electromagnetic currents. Black stars indicate the experimental values, while the blue (red) dots represent the results of calculations including the LO (N³LO) chiral electromagnetic current.

As mentioned earlier, the results presented in this subsection for the

magnetic moments and transition widths of $A = 6-10$ nuclei [111] have been obtained in the hybrid approach, which combines conventional potentials (AV18 and IL7) with chiral electromagnetic currents, see Figs. 11 and 12. Figure 11 makes it plain that the inclusion of corrections beyond LO is necessary in order to have a satisfactory description of the experimental data: their effect is particularly pronounced in the $A = 9$ and isospin $T = 3/2$ systems, in which they provide up to $\sim 20\%$ (40%) of the total predicted value for the ${}^9\text{Li}$ (${}^9\text{C}$) magnetic moments.

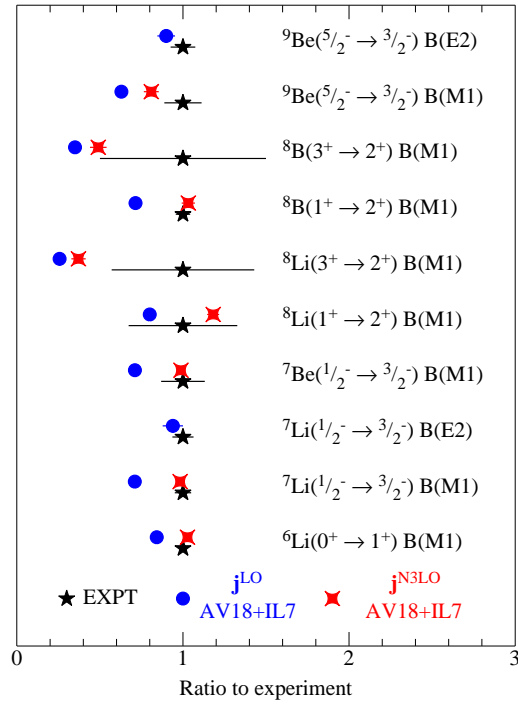


Fig. 12. Ratio to the experimental $M1$ and $E2$ transition widths in $A \leq 9$. Black stars with error bars indicate the experimental values, while the blue dots (red diamonds) represent GFMC AV18/IL7 calculations including chiral electromagnetic currents at LO (up to N3LO).

In Fig. 12 the calculated $M1$ and $E2$ transition widths for $A = 6-9$ nuclei are compared to experimental data. Overall, there is good agreement

between theory and experiment, particularly when one considers the fact that for systems like ${}^8\text{Li}$ and ${}^8\text{B}$ the errors bars are so large to prevent any robust conclusions to be drawn from the apparent under-prediction by theory of the associated widths. It should be noted that the $E2$ widths have been obtained with the LO EM charge operator. Higher order corrections are expected to be very small, in particular the OPE charge operator in Eq. (27) vanishes in the static limit.

4.3. Weak transitions in few-nucleon systems

Most calculations of nuclear axial current matrix elements, such as those discussed below for the pp weak fusion and for muon capture on ${}^2\text{H}$ and ${}^3\text{He}$, have used axial current operators up to N3LO or Q^0 (one exception is Ref. [112], which included effective one-body reductions, for use in a shell-model study, of some of the TPE corrections to the axial current derived in Ref. [35]). A recent application of these N3LO transition operators is the calculation of the rates for μ^- capture on deuteron and ${}^3\text{He}$ [89]. These rates have been predicted with $\sim 1\%$ accuracy,

$$\Gamma({}^2\text{H}) = (399 \pm 3) \text{sec}^{-1}, \quad \Gamma({}^3\text{He}) = (1494 \pm 21) \text{sec}^{-1}.$$

At this level of precision, it is necessary to also account for electroweak radiative corrections, which have been evaluated for these processes in Ref. [113]. The error quoted on the predictions above results from a combination of (i) the experimental error on the ${}^3\text{H}$ GT matrix element used to fix the LEC in the contact axial current, (ii) uncertainties in the electroweak radiative corrections—overall, these corrections increase the rates by 3%—and (iii) the cutoff dependence.

There is a very accurate and precise measurement of the rate on ${}^3\text{He}$: $\Gamma^{\text{EXP}}({}^3\text{He}) = (1496 \pm 4) \text{sec}^{-1}$ [114]. It can be used to constrain the induced pseudo-scalar form factor of the nucleon. It gives $G_{PS}(q_0^2 = -0.95 m_\mu^2) = 8.2 \pm 0.7$, which should be compared to a direct measurement on hydrogen at PSI, $G_{PS}^{\text{EXP}}(q_0^2 = -0.88 m_\mu^2) = 8.06 \pm 0.55$ [115], and a chiral perturbation theory prediction of 7.99 ± 0.20 [116, 117].

The situation for μ^- capture on ${}^2\text{H}$ remains, to this day, somewhat confused: there is a number of measurements that have been carried out, but they all have rather large error bars. However, this unsatisfactory state of affairs should be cleared by an upcoming measurement of this rate by the MuSun collaboration at PSI with a projected 1% error.

Another recent example is the proton weak capture on protons [35, 118]. This process is important in solar physics: it is the largest source

of energy and neutrinos in the Sun. The astrophysical S -factor for this weak fusion reaction is one of the inputs in the standard model of solar (and stellar) evolution [119]. A recent calculation based on N3LO chiral potentials including a full treatment of EM interactions up to order α^2 (α is the fine structure constant), shows that it is now predicted with an accuracy of much less than 1%: $S(0) = (4.030 \pm 0.006) \times 10^{-23} \text{ MeV}\cdot\text{fm}^2$. This calculation also included the (small) effects from capture of the two

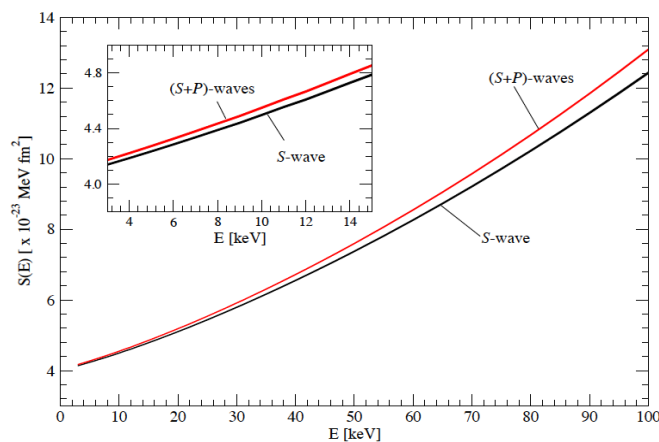


Fig. 13. The S -factor for pp weak fusion due to S- and (S+P)-wave capture as function of energy.

protons in relative P-wave, see Fig. 13 [118]. The increase due to P-wave capture offsets the decrease from higher order EM effects, in particular vacuum polarization.

5. Conclusion

The presentation above illustrates the remarkable progress of the development and application of the chiral Lagrangian based description of nuclear electroweak current operators beginning with the first steps taken by Gerry Brown, Mannque Rho and their colleagues and students around 1970. The early work in the 1970s was, however, based on the lowest order terms in the chiral Lagrangians and, to a large extent, phenomenological wave functions. The advent of systematic chiral effective field theory has brought the theoretical work to a quantitative level and has provided a basis for it in

the fundamental theory of the strong interactions.

We wish to thank our collaborators A. Baroni, J. Carlson, L. Girlanda, A. Kievsky, L.E. Marcucci, S. Pastore, M. Piarulli, S.C. Pieper, M. Viviani, and R.B. Wiringa for their many contributions to the work presented here. The support of the U.S. Department of Energy under contract DE-AC05-06OR23177 is also gratefully acknowledged.

References

- [1] S. Weinberg, *Phys. Rev. Lett.* **17**, 616 (1966).
- [2] G. Brown and J. Durso, *Phys. Lett. B* **35**, 120 (1971).
- [3] M. Chemtob, J. Durso, and D.O. Riska, *Nucl. Phys. B* **38**, 141 (1972).
- [4] M. Chemtob and M. Rho, *Nucl. Phys. A* **163**, 1 (1971).
- [5] M. Chemtob and M. Rho, *Phys. Lett. B* **29**, 540 (1969).
- [6] D.O. Riska and G. Brown, *Phys. Lett. B* **32**, 662 (1970).
- [7] D.O. Riska, *Phys. Scr.* **31**, 471 (1985).
- [8] F. Gross and D.O. Riska, *Phys. Rev. C* **36**, 1928 (1987).
- [9] D.O. Riska and G. Brown, *Phys. Lett. B* **38**, 193 (1972).
- [10] G. Stranahan, *Phys. Rev.* **135**, 953 (1964).
- [11] E. Harper, Y. Kim, A. Tubis, and M. Rho, *Phys. Lett. B* **40**, 533 (1972).
- [12] E. Hadjimichael, *Phys. Rev. Lett.* **31**, 183 (1973).
- [13] I. Towner and F. Khanna, *Nucl. Phys. A* **356**, 445 (1981).
- [14] J. Carlson, D.O. Riska, R. Schiavilla, and R.B. Wiringa, *Phys. Rev. C* **42**, 830 (1990).
- [15] D.O. Riska, *Nucl. Phys. A* **606**, 251 (1996).
- [16] J. Hockert, D.O. Riska, M. Gari, and A. Huffman, *Nucl. Phys. A* **217**, 14 (1973).
- [17] R. Schiavilla and D.O. Riska, *Phys. Rev. C* **43**, 437 (1991).
- [18] R.A. Brandenburg, Y.E. Kim, and A. Tubis, *Phys. Rev. Lett.* **32**, 1325 (1974).
- [19] A. Barroso and E. Hadjimichael, *Nucl. Phys. A* **238**, 422 (1975).
- [20] R. Schiavilla, V.R. Pandharipande, and D.O. Riska, *Phys. Rev. C* **40**, 2294 (1989).
- [21] R.B. Wiringa and R. Schiavilla, *Phys. Rev. Lett.* **81**, 4317 (1998).
- [22] M. Chemtob and A. Lumbroso, *Nucl. Phys. B* **17**, 401 (1970).
- [23] J. Dubach, J. Koch, and T.W. Donnelly, *Nucl. Phys. A* **271**, 279 (1976).
- [24] M. Gari and H. Hyuga, *Phys. Rev. Lett.* **36**, 345 (1976).
- [25] E.M. Nyman and D.O. Riska, *Phys. Rev. Lett.* **57**, 3007 (1986).
- [26] M. Wakamatsu and W. Weise, *Nucl. Phys. A* **477**, 559 (1988).
- [27] L.E. Marcucci, D.O. Riska, and R. Schiavilla, *Phys. Rev. C* **58**, 3069 (1998).
- [28] T.-S. Park, D.-P. Min, and M. Rho, *Phys. Rev. Lett.* **74**, 4153 (1995).
- [29] E. Fischbach, E. Harper, Y. Kim, A. Tubis, and W. Cheng, *Phys. Lett. B* **38**, 8 (1972).

- [30] M. Gari and A. Huffman, *Astrophys. J.* **174**, L153 (1972).
- [31] F. Dautry, M. Rho, and D.O. Riska, *Nuclear Physics A* **264**, 507 (1976).
- [32] R.B. Wiringa, V.G.J. Stoks, and R. Schiavilla, *Phys. Rev. C* **51**, 38 (1995).
- [33] J. Carlson, D.O. Riska, R. Schiavilla, and R.B. Wiringa, *Phys. Rev. C* **44**, 619 (1991).
- [34] T.-S. Park, K. Kubodera, D.-P. Min, and M. Rho, *Astrophys. J.* **507**, 443 (1998).
- [35] T.-S. Park, L.E. Marcucci, R. Schiavilla, M. Viviani, A. Kievsky, S. Rosati, K. Kubodera, D.-P. Min, and M. Rho, *Phys. Rev. C* **67**, 055206 (2003).
- [36] W. Kloet and J. Tjon, *Phys. Lett. B* **49**, 419 (1974).
- [37] J. Borysowicz and D.O. Riska, *Nucl. Phys. A* **254**, 301 (1975).
- [38] R. Schiavilla, V.R. Pandharipande, and D.O. Riska, *Phys. Rev. C* **41**, 309 (1990).
- [39] M. Radomski and D.O. Riska, *Nucl. Phys. A* **274**, 428 (1976).
- [40] A. Lovato, S. Gandolfi, R. Butler, J. Carlson, E. Lusk, S.C. Pieper, and R. Schiavilla, *Phys. Rev. Lett.* **111**, 092501 (2013).
- [41] J.W. Negele and D.O. Riska, *Phys. Rev. Lett.* **40**, 1005 (1978).
- [42] D. Abbott *et al.*, *Eur. Phys. J. A* **7**, 421 (2000).
- [43] D.O. Riska and M. Radomski, *Phys. Rev. C* **16**, 2105 (1977).
- [44] M. Kirchbach, R. Mach, and D.O. Riska, *Nucl. Phys. A* **511**, 592 (1990).
- [45] M. Kirchbach, D.O. Riska, and K. Tsushima, *Nucl. Phys. A* **542**, 616 (1992).
- [46] I. Towner, *Nucl. Phys. A* **542**, 631 (1992).
- [47] E.K. Warburton, *Phys. Rev. Lett.* **66**, 1823 (1991).
- [48] T.-S. Park, D.-P. Min, and M. Rho, *Phys. Rep.* **233**, 341 (1993).
- [49] T.-S.H. Lee and D.O. Riska, *Phys. Rev. Lett.* **70**, 2237 (1993).
- [50] G. Brown and M. Rho, *Phys. Lett. B* **82**, 177 (1979).
- [51] G. Brown, A. Jackson, M. Rho, and V. Vento, *Phys. Lett. B* **140**, 285 (1984).
- [52] E. Witten, *Nucl. Phys. B* **160**, 57 (1979).
- [53] E.M. Nyman and D.O. Riska, *Nucl. Phys. A* **468**, 473 (1987).
- [54] U. Blom and D.O. Riska, *Nucl. Phys. A* **476**, 603 (1988).
- [55] S. Weinberg, *Phys. Lett. B* **251**, 288 (1990).
- [56] S. Weinberg, *Nucl. Phys. B* **363**, 3 (1991).
- [57] S. Weinberg, *Phys. Lett. B* **295**, 114 (1992).
- [58] C. Ordonez, L. Ray, and U. van Kolck, *Phys. Rev. C* **53**, 2086 (1996).
- [59] E. Epelbaum, W. Gloeckle, and U. G. Meissner, *Nucl. Phys. A* **637**, 107 (1998).
- [60] D. Entem and R. Machleidt, *Phys. Rev. C* **68**, 041001 (2003).
- [61] R. Machleidt and D. Entem, *Phys. Rep.* **503**, 1 (2011).
- [62] P. Navratil, *Few-Body Syst.* **41**, 117 (2007).
- [63] E. Epelbaum *et al.*, *Phys. Rev. C* **66**, 064001 (2002).
- [64] U. van Kolck, *Phys. Rev. C* **49**, 2932 (1994).
- [65] V. Bernard, E. Epelbaum, H. Krebs, and U.-G. Meissner, *Phys. Rev. C* **84**, 054001 (2011).
- [66] L. Girlanda, A. Kievsky, and M. Viviani, *Phys. Rev. C* **84**, 014001 (2011).

- [67] J. L. Friar and U. van Kolck, *Phys. Rev. C* **60**, 034006 (1999).
- [68] E. Epelbaum and U. G. Meissner, *Phys. Lett. B* **461**, 287 (1999).
- [69] J. L. Friar, U. van Kolck, M. C. M. Rentmeester, and R. G. E. Timmermans, *Phys. Rev. C* **70**, 044001 (2004).
- [70] J. L. Friar, G. L. Payne, and U. van Kolck, *Phys. Rev. C* **71**, 024003 (2005).
- [71] W. C. Haxton and B. R. Holstein, *Prog. Part. Nucl. Phys.* **71**, 185 (2013).
- [72] S. L. Zhu, C. M. Maekawa, B. R. Holstein, M. J. Ramsey-Musolf, and U. van Kolck, *Nucl. Phys. A* **748**, 435 (2005).
- [73] L. Girlanda, *Phys. Rev. C* **77**, 067001 (2008).
- [74] M. Viviani, A. Baroni, L. Girlanda, A. Kievsky, L. E. Marcucci, and R. Schiavilla, *Phys. Rev. C* **89**, 064004 (2014).
- [75] V. Pascalutsa and D.R. Phillips, *Phys. Rev. C* **67**, 055202 (2003).
- [76] H. Griesshammer, J. McGovern, D.R. Phillips, and G. Feldman, *Prog. Part. Nucl. Phys.* **67**, 841 (2012).
- [77] T.-S. Park, D.-P. Min, and M. Rho, *Nucl. Phys. A* **596**, 515 (1996).
- [78] S. Pastore, L. Girlanda, R. Schiavilla, M. Viviani, and R. Wiringa, *Phys. Rev. C* **80**, 034004 (2009).
- [79] S. Pastore, L. Girlanda, R. Schiavilla, and M. Viviani, *Phys. Rev. C* **84**, 024001 (2011).
- [80] M. Piarulli, L. Girlanda, L. Marcucci, S. Pastore, R. Schiavilla, and M. Viviani, *Phys. Rev. C* **87**, 014006 (2013).
- [81] A. Baroni, L. Girlanda, S. Pastore, R. Schiavilla, and M. Viviani, *Phys. Rev. C* **93**, 015501 (2016).
- [82] S. Kölling, E. Epelbaum, H. Krebs, and U.-G. Meissner, *Phys. Rev. C* **80**, 045502 (2009).
- [83] S. Kölling, E. Epelbaum, H. Krebs, and U.-G. Meissner, *Phys. Rev. C* **84**, 054008 (2011).
- [84] J. Gasser and H. Leutwyler, *Annals of Physics* **158**, 142 (1984).
- [85] N. Fettes, U.-G. Meissner, M. Mojzsis, and S. Steininger, *Ann. Phys. (N.Y.)* **283**, 273 (2000).
- [86] L. Girlanda, S. Pastore, R. Schiavilla, and M. Viviani, *Phys. Rev. C* **81**, 034005 (2010).
- [87] A. Gärdestig and D.R. Phillips, *Phys. Rev. Lett.* **96**, 232301 (2006).
- [88] D. Gazit, S. Quaglioni, and P. Navrátil, *Phys. Rev. Lett.* **103**, 102502 (2009).
- [89] L.E. Marcucci, A. Kievsky, S. Rosati, R. Schiavilla, and M. Viviani, *Phys. Rev. Lett.* **108**, 052502 (2012).
- [90] S. Pastore, R. Schiavilla, and J.L. Goity, *Phys. Rev. C* **78**, 064002 (2008).
- [91] S. Okubo, *Prog. Theor. Phys.* **12**, 603 (1954).
- [92] D.R. Phillips, *Phys. Lett. B* **567**, 12 (2003).
- [93] D. O. Riska, *Phys. Rep.* **181**, 207 (1989).
- [94] J. Carlson and R. Schiavilla, *Rev. Mod. Phys.* **70**, 743 (1998).
- [95] K. Kubodera, J. Delorme, and M. Rho, *Phys. Rev. Lett.* **40**, 755 (1978).
- [96] E. Epelbaum, H. Krebs, and U. G. Meissner, *Phys. Rev. Lett.* **115**, 122301 (2015).
- [97] E. Epelbaum, A. Nogga, W. Glöckle, H. Kamada, U.-G. Meißner, and

- H. Witała, *Phys. Rev. C* **66**, 064001 (2002).
- [98] L. Girlanda, A. Kievsky, L. Marcucci, S. Pastore, R. Schiavilla, and M. Viviani, *Phys. Rev. Lett.* **105**, 232502 (2010).
- [99] J. Carlson, S. Gandolfi, F. Pederiva, S. C. Pieper, R. Schiavilla, K. Schmidt, and R. Wiringa, *Rev. Mod. Phys.* **87**, 1067 (2015).
- [100] S. Kölling, E. Epelbaum, and D.R. Phillips, *Phys. Rev. C* **86**, 047001 (2012).
- [101] S. Bacca and S. Pastore, *J. Phys. G: Nucl. Part. Phys.* **41**, 123002 (2014).
- [102] L. E. Marcucci, F. Gross, M. T. Pea, M. Piarulli, R. Schiavilla, I. Sick, A. Stadler, J. W. V. Orden, and M. Viviani, *J. Phys. G: Nucl. Part. Phys.* **43**, 023002 (2016).
- [103] D.R. Phillips, *J. Phys. G: Nucl. Part. Phys.* **34**, 365 (2007).
- [104] A. Camsonne *et al.*, *Phys. Rev. Lett.* **112**, 132503 (2014).
- [105] F. Gross, *Phys. Rev. C* **91**, 014005 (2015).
- [106] A. Kievsky, S. Rosati, M. Viviani, L.E. Marcucci, and L. Girlanda, *J. Phys. G: Nucl. Part. Phys.* **35**, 063101 (2008).
- [107] E. T. Jurney, P. J. Bendt, and J. C. Browne, *Phys. Rev. C* **25**, 2810 (1982).
- [108] F.L.H. Wolfs, S.J. Freedman, J.E. Nelson, M.S. Dewey, and G.L. Greene, *Phys. Rev. Lett.* **63**, 2721- (1989).
- [109] R. Wervelman, K. Abrahams, H. Postma, J. Booten, and A.V Hees, *Nucl. Phys. A* **526**, 265 (1991).
- [110] M. Piarulli, L. Girlanda, R. Schiavilla, R.N. Pérez, J.E. Amaro, and E.R. Arriola, *Phys. Rev. C* **91**, 024003 (2015).
- [111] S. Pastore, S.C. Pieper, R. Schiavilla, and R.B. Wiringa, *Phys. Rev. C* **87**, 035503 (2013).
- [112] P. Klos, J. Menéndez, D. Gazit, and A. Schwenk, *Phys. Rev. D* **88**, 083516 (2013).
- [113] A. Czarnecki, W.J. Marciano, and A. Sirlin, *Phys. Rev. Lett.* **99**, 032003 (2007).
- [114] P. Ackerbauer *et al.*, *Phys. Lett. B* **417**, 224 (1998).
- [115] V. A. Andreev *et al.*, *Phys. Rev. Lett.* **110**, 012504 (2013).
- [116] V. Bernard, N. Kaiser, and U.-G. Meissner, *Phys. Rev. D* **50**, 6899 (1994).
- [117] N. Kaiser, *Phys. Rev. C* **67**, 027002 (2003).
- [118] L. E. Marcucci, R. Schiavilla, and M. Viviani, *Phys. Rev. Lett.* **110**, 192503 (2013).
- [119] J.N. Bahcall and M.H. Pinsonneault, *Phys. Rev. Lett.* **92**, 121301 (2004).